Desalination and Water Treatment
www.deswater.com
1944-3994/1944-3986 © 2012 Desalination Publications. All rights reserved
doi: 10/5004/dwt.2012.1133

37(2012)200–214
January

Taylor & Francis
Taylor & Francis Group

Kinetics of the batch adsorption of methylene blue from aqueous solutions onto rice husk: effect of acid-modified process and dye concentration

Ming-Cheng Shih

Department of Biological Science and Technology, I-Shou University, No.8, Yida Rd., Jiaosu Village, Yanchao District, Kaohsiung City 82445, Taiwan, R.O.C.
Tel. +886-7-6151100 ext. 7321; Fax: +886-7-6577056; email: mchshih@isu.edu.tw

Received 30 March 2010; Accepted 5 July 2011

ABSTRACT

In this study, adsorption of methylene blue (MB) dye onto clean rice husks (CRH) and acid-modified CRH was investigated with respect to the contact time, MB concentrations, acid concentrations and acid types used in the acid modification processes. The results indicate that the acid modification process reduces the MB sorption efficiency from 98% for CRH to 67% for NRH (nitric acid treated rice husk), 59% for HRH (hydrochloric acid treated rice husk) and 55% for SRH (sulfuric acid treated rice husk). In order to investigate the adsorption mechanisms, four kinetic models, i.e., pseudo-first-order, pseudo-second-order, Elovich and intraparticle diffusion models were fit to the experimental results. The characteristic parameters and correlation coefficients for each kinetic model were determined. The fits of the kinetic results from the kinetic equations were compared with the experimental data. The results indicate that the acid modification process changes the MB adsorption mechanism. Langmuir, Freundlich, Temkin, Redlich-Peterson (RP), and Langmuir-Freundlich (LF) isotherm models were also employed to analyze the equilibrium data, and the correlations of the experimental data to the isotherms was examined. The LF isotherm was found to best represent the data for MB adsorption onto CRH. The separation factor revealed the favorable nature of the isotherm to the MB-CRH system.

Keywords: Acid-modified; Methylene blue; Adsorption; Kinetics; Equilibrium isotherms; Rice Husk

1. Introduction

Many industries, such as the cosmetics, leather, carpet, dye manufacturing and textile finishing industries, use dyes to color their products. They also consume a lot of clean water, which becomes colored wastewater, poured into the environment where trade wastewater measures are not in place [1,2]. The effluents of these industries can cause local environmental problems by significantly affecting photosynthetic activity in aquatic life because of the reduced light penetration. The effluents may also be toxic to some forms of aquatic life because of the presence of metals, chlorides, etc., in them [3,4]. In addition, introducing dye compounds into the aquatic environment is aesthetically displeasing. Because of these negative impacts, there is a need to develop decolorization methods that are effective and suitable for industrial use. Currently, the major methods for dye and color removal involve microbial, physical and/or chemical processes, such as microbial degradation, chemical oxidation, and membrane separation process have been proposed from time to time [5–10]. However, all of the current methods suffer from one limitation or another, and none have been successful in removing color from wastewater completely. Adsorption is probably the simplest process for dye removal. Currently, activated carbon is believed to be the most effective adsorbent and is the most popular

physicochemical treatment for the removal of dissolved dyes from wastewaters [4]; however, its manufacturing and regeneration costs are high [11]. In order to reduce the cost of an adsorption system, some attempts have been made to find low cost alternative adsorbents. A wide variety of materials such as *Aspergillus niger* biomass, algal biomass, *Spirogyra rhizopus* biomass, rice husk, bark, wheat shell, citric acid esterifying wheat straw, dehydrated wheat bran, carbonized press mud, tree fern, apple pomace and wheat straw, coir pith, cotton, mango seed kernel, shell of bittim, banana stalk waste, dolomitic sorbents, chitosan, wood sawdust, palm kernel fiber, jute fiber, waste of sugarcane, perlite, raw kaolin, pure kaolin, calcined rawkaoline, calcined pure kaolin, NaOH treated raw kaolin, palygorskite, zeolite, and surfactant-modified activated carbon have been investigated with varying degrees of success [1,2,4][12–34].

In the present study, rice husks (an agro-residue) have been investigated as an adsorbent for the removal of methylene blue from aqueous solutions. Rice husks, a by-product of the rice milling industry, account for about 20% of rice as a whole [35]. With an estimated annual rice production of 500 million metric tons in developing countries, approximately 100 million tons of rice husks are available annually for utilization in these countries alone. In fact, the amount of rice husks available is far in excess of any local uses and, thus, has posed disposal problems. Rice husks were chosen for investigation as a precursor material due to their granular structure, insolubility in water, chemical stability, high mechanical strength and local availability at almost no cost [35]. The advantage in the use of these adsorbents is that there is no need to regenerate them because of their low production costs. In the present study, the effects of the contact time, the acid concentration in the acid modification process, the type of acid used in the acid modification process, and the initial methylene blue (MB) concentration on the amount of color removed have been investigated. In order to investigate the mechanism of adsorption, experimental data was modeled using the pseudo-first-order, pseudo-second-order, Elovich and intraparticle diffusion models. Equilibrium isotherms were analyzed according to the Langmuir isotherm; the Freundlich, Temkin, Redlich–Peterson and Langmuir–Freundlich isotherms were only analyzed for the adsorbent exhibiting the highest MB removal efficiency. The characteristic parameters for each model were determined.

2. Materials and methods

2.1. Preparation of adsorbent

The rice husk used in the present investigation was obtained from local rice mills in Taiwan. The whole rice husk was used; the integrity and the size of rice husk were not modified. The collected materials were washed with water several times to remove dust and fines, the washing process continued until the wash water contained no color. It was subsequently rinsed several times with reverse osmosis (RO) water and dried overnight in an oven at 85±3°C. The sorbent thus obtained was termed clean rice husk (CRH). The CRH was then stored in plastic bottles and used for biosorption studies, the individual husks still in their original sizes.

Preliminary studies using CRH treated with various types of acid were carried out in order to evaluate the possibility of optimizing the sorption of dyes. The CRH was soaked in 0.75 M nitric acid at a ratio of 1:10 (CRH: nitric acid, w/v) for four hours at room temperature. The nitric acid-treated CRH (termed NRH) was washed thoroughly with water to remove residual acid and then dried overnight in an oven at 85±3°C. Similar acid treatments were also performed with hydrochloric acid (making HRH) and sulfuric acid (making SRH). The yields of the three pretreated rice husks were essentially the same (97–98% w/w of the original dry material). Different sulfuric acid concentrations (0 M, 0.75 M, and 3 M) were used in the acid modification process to evaluate the effect of the acid concentration on the amount of color removal. The yields of the pretreated rice husks were approximately equal (94–97% w/w of the original dry material) under the three sulfuric acid concentrations.

2.2. Dye solution preparation

The cationic dye 'methylene blue' was chosen in this study as a model molecule for basic dyes. Stock solutions of MB were prepared by dissolving accurately weighed samples of dye in distilled water to give a concentration of 1000 mg/l. The experimental solutions were prepared by diluting, where necessary, the dye stock solution (1000 ppm) with RO water to the required concentrations. All the experiments were conducted at a natural pH (6.8–7.1) without any pH adjustment.

2.3. Batch adsorption experiments

Sorption tests on the acid-modified and natural rice husks were performed in order to determine the time needed to reach equilibrium and the pattern of the kinetics. For this purpose, samples of 2 g of natural or acid-modified rice husks were transferred into bottles containing 100 ml of 50 mg/l MB solution. The bottles were placed at 25±2°C using a temperature controlled shaker operating at 125 rpm. The samples were taken from the shaker at predetermined time intervals. The residual concentration of MB at any time, t,

was determined from absorbency as measured with a UV-Vis spectrophotometer (Hitachi, U–1800) at a 660 nm wavelength, at which the maximum absorbency occurred.

The effect of the initial dye concentrations on the amount of MB adsorbed was examined by contacting 2 g samples of CRH with 100 ml quantities of MB solution of different initial dye concentrations, varying from 10 to 100 mg/l. All experiments were conducted at 25±2°C using a temperature controlled shaker operating at 125 rpm. The samples were taken from the shaker at predetermined time intervals.

The amount of dye adsorbed at time t and the amount of dye adsorbed at equilibrium time, are calculated by Eq. (1) and Eq. (2) [36]:

$$\text{Amount of methylene blue adsorbed at time } t\ (q_t) = \frac{(C_i - C_t)V}{M} \quad (1)$$

$$\text{Amount of methylene blue adsorbed at equilibrium } (q_e) = \frac{(C_i - C_e)V}{M} \quad (2)$$

where C_i, C_t and C_e (mg/l) are the liquid phase concentrations of dyes initially, at time t and at equilibrium time, respectively, V is the volume of dye solution (l), and M is the weight of adsorbent used (g).

2.4. Kinetics of adsorption

The kinetics of adsorption is one of the most important characteristics in defining the efficiency of adsorption, hence the examination of the kinetics of MB adsorption in this study. Four kinds of kinetic models, the pseudo-first-order kinetic, pseudo-second-order kinetic, Elovich and intraparticle diffusion models have been tested to analyze the experimental data. All the model parameters were evaluated by nonlinear regression.

2.4.1. The pseudo-first-order kinetic model

The pseudo-first-order equation is the most popular kinetic equation. The form is expressed as follows [37]:

$$\frac{dq_t}{dt} = K_1(q_e - q_t) \quad (3)$$

After definite integration by applying the boundary conditions $t = 0$ to $t = t$ and $q_t = 0$ to $q_t = q_t$, the integrated form of Eq. (3) becomes the following [38]:

$$q_t = q_e\left(1 - \exp\left(-K_1 t\right)\right) \quad (4)$$

where q_t (mg/g) is the amount of adsorption time t (min); K_1, the rate constant of the pseudo-first-order equation (min^{-1}) and q_e is the amount of adsorption equilibrium (mg/g).

2.4.2. The pseudo- second-order kinetic model

The second order is based on the adsorption capacity: it can predict the adsorption behavior only over a certain range determined by prior study, but is in agreement with previous studies which suggest chemisorption controls the adsorption rate [39,40]. The pseudo-second-order adsorption kinetic rate equation of Ho and McKay is expressed as [41,42]:

$$\frac{dq_t}{dt} = K_2(q_e - q_t)^2 \quad (5)$$

where q_t (mg/g) is the amount of adsorption time t (min); K_2, the rate constant of the pseudo-second-order equation (min^{-1}) and q_e is the amount of adsorption equilibrium (mg/g). Integrating Eq. (5) for the boundary conditions $t = 0$ to $t = t$ and $q_t = 0$ to $q_t = q_t$ gives [43]:

$$\frac{1}{(q_e - q_t)} = \frac{1}{q_e} + K_2 t \quad (6)$$

which is the integrated rate law for a pseudo-second-order reaction. For non-linear, the equation can be written as [38]:

$$q_t = \left(\frac{K_2 q_e^2 t}{1 + K_2 q_e t}\right) \quad (7)$$

2.4.3. The Elovich model

In reactions involving chemisorption of adsorbate onto a solid surface without desorption of products, the adsorption rate decreases with time due to an increased surface coverage. One of the most useful models for describing such 'activated' chemisorption is the Elovich equation [38]. The Elovich equation assumes that the active sites of the biosorbent are heterogeneous and therefore exhibit different activation energies for chemisorption. The Elovich model equation is generally expressed as [44,45]:

$$\frac{dq_t}{dt} = \alpha \exp(-\beta q_t) \quad (8)$$

where q_t is the sorption capacity at time t (mg/g); α is the initial adsorption rate (mg/g min) because dq_t/dt approaches α when q_t approaches zero; and β is the desorption constant (g/mg) during any one experiment.

Given that $q_t = 0$ at $t = 0$, the integrated form of Eq. (8) becomes:

$$q_t = \frac{1}{\beta}\ln(t + t_o) - \frac{1}{\beta}\ln(t_o) \quad (9)$$

where $t_0 = 1/\alpha\beta$. If t is much larger than t_0, Eq. (9) can be simplified to:

$$q_t = \frac{1}{\beta}\ln(\alpha\beta) + \frac{1}{\beta}\ln(t) \quad (10)$$

2.4.4. The intraparticle diffusion model

In a solid–liquid adsorption process, the adsorption dynamics generally consist of three main consecutive transport steps: (i) transport of dye molecules from the bulk solution to the external surface of the adsorbent by diffusion through the liquid boundary layer (film diffusion); (ii) diffusion of the dye from the external surface and into the pores of the adsorbent (intraparticle diffusion); and (iii) adsorption of the dye onto the active sites of the internal surface of the pores (pore diffusion) [46]. Among the three steps, the last step is considered to have a negligible effect on kinetics, as it is assumed to be rapid. The rate of absorption is controlled by either film diffusion or pore diffusion, depending on which step is slower [47].

Accordingly, the overall rate of adsorption is controlled by either film or intraparticle diffusion, or a combination of both. Many studies have shown that boundary layer diffusion is dominant during the initial adsorbate uptake, after which the adsorption rate gradually becomes controlled by intraparticle diffusion as the adsorbent's external surface is loaded with the adsorbate [46,47]. The intraparticle diffusion model is expressed as [48,49]:

$$q_t = K_{id} t^{\frac{1}{2}} + C \quad (11)$$

where q_t is the sorption capacity at time t (mg/g); C is the intercept; and K_{id} is the intraparticle diffusion rate constant (mg/g $\text{min}^{-1/2}$). Thus, the intraparticle diffusion constant K_{id}, can be obtained from the slope of the plot of q_t versus the square root of time. If the regression of q_t versus $t^{0.5}$ is linear and passes through the origin, then intraparticle diffusion is the sole rate-limiting step; if not, the boundary layer diffusion controls the adsorption to some degree and this indicated that the intraparticle diffusion is not the only rate controlling step, but also other processes may control the rate of adsorption.

2.5. Adsorption isotherms

An adsorption isotherm shows the equilibrium relationship between concentration in the solution and the quantity of adsorbate adsorbed at constant temperature. They provide fundamental physiochemical data about the sorption process, and may be used for scaling-up batch type processes with moderate success. The shape of the equilibrium adsorption isotherm provides information about the homogeneity and heterogeneity of the adsorbent surface [50,51]. In the present investigation, the equilibrium data were analyzed using five equilibrium models, the Langmuir, Freundlich, Temkin, the Redlich–Peterson (RP), and the Langmuir–Freundlich (LF) isotherms for describing solid–liquid sorption systems. In this study, the equilibrium adsorption isotherms were only applied to the adsorbent which had the highest MB removal efficiency. All the model parameters were evaluated by nonlinear regression.

2.5.1. Langmuir isotherm

The Langmuir adsorption isotherm model assumes that adsorption occurs on a homogenous adsorbent surface of identical sites that are equally available and energetically equivalent, with each site carrying an equal number of adsorbed molecules, and no interaction between adsorbate molecules [51–53]. The saturated monolayer isotherm can be represented as:

$$q_e = \frac{q_{max} K_L C_e}{1 + K_L C_e} \quad (12)$$

where q_e is the amount of MB adsorbed on adsorbent at equilibrium (mg/g), C_e is the equilibrium concentration in the solution (mg/l), q_{max} is the q_e for a complete monolayer (mg/g), a constant related to the sorption capacity, and K_L is the adsorption equilibrium constant related to the affinity of the binding sites and the energy of adsorption (l/mg). For Langmuir type adsorption processes, the influence of the isotherm shape on whether adsorption is "favorable" or "unfavorable" can be classified by a term "R_L" a dimensionless constant separation factor [54].

$$R_L = \frac{1}{1 + k_L C_i} \quad (13)$$

where C_i (mg/l) is the liquid phase initial concentration of the dye. The R_L parameter is considered a reliable indicator of the adsorption. There are four probabilities for the R_L value: (i) for favorable adsorption, $0 < R_L < 1$, (ii) for unfavorable adsorption, $R_L > 1$, (iii) for linear adsorption, $R_L = 1$, and (iv) for irreversible adsorption, $R_L = 0$ [52].

2.5.2. Freundlich isotherm

The Freundlich isotherm assumes that the adsorption occurs on a heterogeneous surface at non-identical sites with different energies of adsorption that are not always available. This fairly satisfactory empirical isotherm can be used for non-ideal sorption and is expressed by the following equation [50, 55–56]:

$$q_e = K_F C_e^{\frac{1}{n}} \quad (14)$$

where K_F is an indicator of the relative adsorption capacity of the adsorbent ($mg^{1-(1/n)}\,l^{1/n}/g$); and n is that of the adsorption intensity, respectively.

In order to determine the maximum adsorption capacity, it is necessary to operate with a constant initial concentration C_i and variable amounts of adsorbent; ln q_{max} is then the extrapolated value of ln q for $C = C_i$ [57].

$$K_F = \frac{q_{max}}{C_i^{\frac{1}{n}}} \quad (15)$$

where C_i (mg/l) is the liquid phase concentrations of dyes initially and q_{max} is the Freundlich maximum adsorption capacity (mg/g).

2.5.3. Temkin isotherm

The derivation of the Temkin isotherm assumes that the fall in the heat of sorption is linear rather than logarithmic, as implied in the Freundlich equation. The heat of sorption of all the molecules in the layer is assumed to decrease linearly with coverage due to sorbate/sorbent interactions [58]. The Temkin isotherm has generally been applied in the following form:

$$q_e = \frac{RT}{B_T} \ln\left(A_T C_e\right) \quad (16)$$

where B_T is the Temkin constant, related to the heat of sorption (J/mol); A_T is the Temkin isotherm constant (l/g); R is the gas constant (8.314 J/mol K); and T is the absolute temperature in K.

2.5.4. Redlich–Peterson isotherm

The Redlich–Peterson isotherm contains three parameters and incorporates the features of the Langmuir and Freundlich isotherms. It can be represented by the following formula [51]:

$$q_e = \frac{K_R C_e}{1 + A C_e^{\,b}} \quad (17)$$

where C_e (mg/l) is the equilibrium concentration in the solution; K_R (l/g) and A ($(l/mg)^b$) are the Redlich-Peterson constants; and b is the Redlich-Peterson isotherm exponent. In this study all the model parameters were calculated by nonlinear regression.

2.5.5. Langmuir–Freundlich (LF) isotherm

The Langmuir–Freundlich (LF) isotherm, derived from the Langmuir and Freundlich models, is a three-parameter empirical model represented by the following equation [59]:

$$q_e = \frac{q_{LF} K_{LF} C_e^{\frac{1}{n}}}{1 + K_{LF} C_e^{\frac{1}{n}}} \quad (18)$$

where K_{LF} is the equilibrium constant ($(l/mg)^{1/n}$), q_{LF} is the maximum amount of dye per unit weight of biosorbent (mg/g), and n is an empirical dimensionless parameter. If $n = 1$, Eq. (18) becomes the Langmuir equation. This model is valid when $l/n > 1$. In this study the isotherm parameters of LF equation were evaluated using nonlinear regression.

3. Results and discussion

3.1. FTIR spectroscopy studies

The Fourier transform infrared (FT-IR) spectroscopy technique is an important tool for identifying characteristic functional groups which are capable of adsorbing metal ions and dye ions. The raw material and acid-modified adsorbent were characterized using a FT-IR spectrophotometer (PerkinElmer, Spectrum RX1) at room temperature (Fig. 1). As seen in Fig. 1, the presence of OH groups on the surface of the rice husks is confirmed by a broad band between 3300 and 3450 cm^{-1} [60]. This stretching of OH groups is associated to silanol groups (Si–OH) and to adsorbed water on the

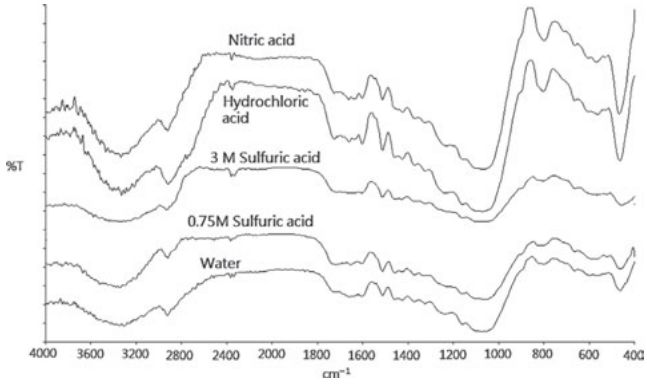

Fig. 1. FTIR spectra for CRH, SRH, HRH, NRH.

rice husks' surfaces. Other OH groups bound to methyl radicals exhibited a signal between 2920 and 2940 cm^{-1} [60]. These groups are common in lignin structures. The peaks located at 1640 to 1670 cm^{-1} are characteristic of carbonyl stretching from aldehydes and ketones [61]. The peaks associated with the stretching of aromatic rings were verified at 1511 cm^{-1} [60]. The bands between 1130–1050 and 810–800 cm^{-1} were attributed to O–Si–O and typical structures of SiO2, which was an indication of silica [62]. Finally, the presence of a band around 466 cm^{-1} is generally attributable to the bending vibration of O–Si–O [62].

3.2. Effect of acid concentration on sorption and sorption kinetics

Fig. 2 shows the effect of the acid concentration and the contact time on the amount of MB adsorbed onto H_2SO_4 modified rice husks. It was observed that the chemical modification resulted in a decrease of the sorption capacities of the CRH.

In order to analyze the MB biosorption kinetics, the pseudo-first-order kinetic, pseudo-second-order kinetic, Elovich, and intraparticle diffusion kinetic models were applied to the data. The fittings of the pseudo-first-order kinetic model to the experimental results are shown in Fig. 2a, and the values of the estimated parameters are presented in Table 1. The resulting curves and data obtained by the pseudo-first-order kinetic equation did not describe the biosorption of the dye on the CRH well. It was noticed, also, that curves of fit for the H_2SO_4 modified CRH were closer to the experimental values than the curve of fit for the CRH. These results indicated that the modification of CRH could destroy the structure of the adsorption surface and affect the mechanisms of adsorption.

The comparisons of the calculated results for the pseudo-second-order kinetic model and the measured results for the CRH and acid-modified CRHs are shown in Fig. 2b. As observed in Fig. 2b, the pseudo-second-order expression better predicted the sorption kinetics than the pseudo-first-order model for the entire sorption

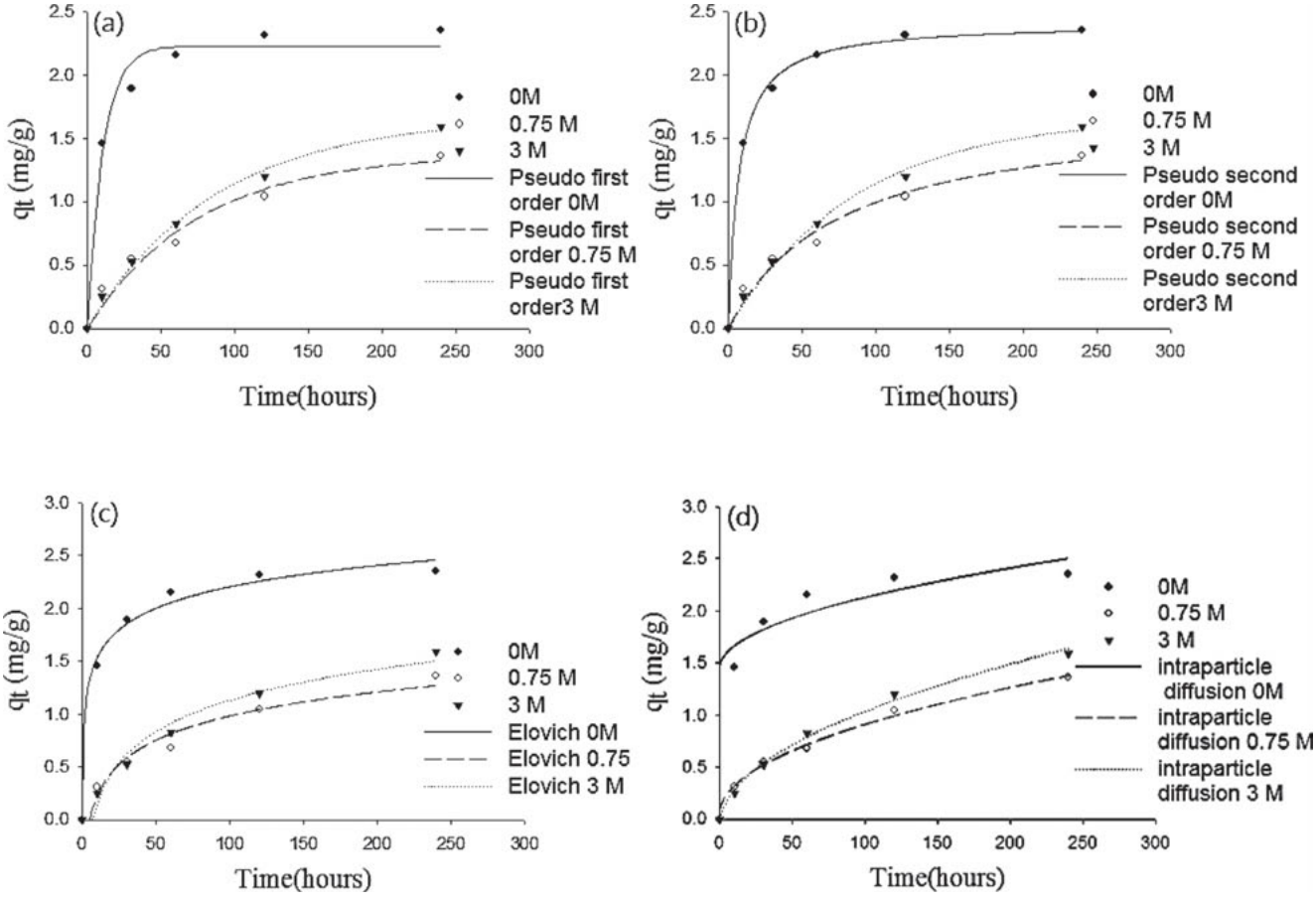

Fig. 2. Comparison between the measured and modeled time profiles and comparison of kinetic models in predicting q_t for the adsorption of MB onto CRHs modified by various acid concentrations.

Table 1
Kinetic parameters of the removal of MB from aqueous solution by the CRHs modified by various acid concentrations

Acid concentration	Pseudo-first-order			Pseudo-second-order				Elovich equation			Intraparticle diffusion		
	*K*1	q_e	r^2	*K*2	q_e	*h*	r^2	α	β	r^2	K_{id}	*C*	r^2
0M	0.0941	2.2281	0.98	0.0596	2.4098	0.3455	0.9982	5.6763	3.4382	0.9433	0.0679	1.4499	0.7893
0.75M	0.0134	1.3731	0.9679	0.0076	1.7424	0.0516	0.9797	0.0650	3.0398	0.9489	0.0858	0.0513	0.992
3M	0.0115	1.6710	0.9943	0.0045	2.24	0.0224	0.9982	0.0605	2.3507	0.9698	0.1098	–0.0634	0.993

period, especially for CRH. This suggested the pseudo-second-order kinetic model could be used to predict the dye uptake amount at different contact time intervals and at equilibrium for CRH and H_2SO_4 modified CRH.

The experimental data and the simulations using the Elovich equation for modeling the adsorption of MB onto different absorbents are shown in Fig. 2c. The fits are not as good as the pseudo-second-order models. As for the pseudo-first-order model, the curves of fit for H_2SO_4 modified CRH were closer to the experimental values than the curves of fit for CRH. The constants for the Elovich equation for the same experimental data were obtained from the slope and intercept of the plot of q_t against ln *t* (plot not shown), listed in Table 1. When using the Elovich equation, the constant α represents the initial adsorption rate, while β is related to the extent of the surface coverage and the activation energy involved in chemisorption [63]. It was observed that α and β decreased as the acid concentration increased (Table 1). This suggests that the adsorption surface of the absorbents was affected such that the available adsorption sites lessened as the acid concentration increased.

The simulations using the intraparticle diffusion equation for the adsorption of MB onto the different absorbents are shown in Fig. 2d. The intraparticle diffusion model expression did not fit well with the experimental data for the CRH. This suggested the intraparticle diffusion model could not be used to predict the amount of dye uptake at different contact time intervals and at equilibrium for CRH. However, a good fit was produced for the experimental data for H_2SO_4 modified CRH, almost as good as the pseudo-second-order model. These results again indicated that the acid modification of CRH could destroy the structure of the adsorption surface and affect the mechanisms of adsorption.

The adsorption process for MB onto CRH is mainly controlled by diffusion from the solid-liquid interface towards the solid particles. This mechanism may be tested by plotting q_t versus $t^{0.5}$ (Fig. 3). As shown, the adsorption process for CRH was not linear over the whole time range and tended to be in two phases. The initial curved portion is attributable to the boundary layer diffusion effects and the final linear portion may be due to the intraparticle diffusion effects. Also, the linear plot

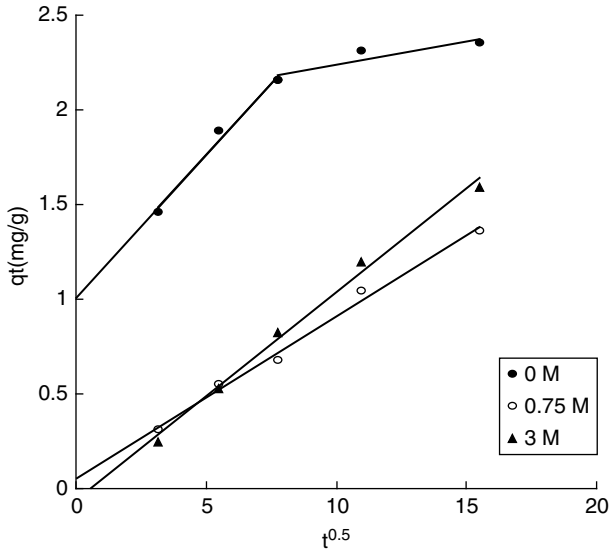

Fig. 3. Intraparticle diffusion plot for the adsorption of MB onto CRHs modified by various acid concentrations.

for the non-modified CRH does not pass through the origin, which indicates that intraparticle diffusion was not the only rate controlling step. However, the linear plots for each acid-modified absorbent pass through very close to the origin, indicating that intraparticle diffusion plays a major role in the adsorption for acid-modified absorbents.

3.3. Effect of chemical treatment on sorption and sorption kinetics

The chemical treatment of CRH was shown to result in certain changes in its surface properties. Accordingly, the MB adsorption behavior for each of the acid-modified CRHs was more closely examined. Fig. 4 shows the effect of the chemical treatment and the contact time on the amount of MB adsorbed onto H_2SO_4 modified rice husks. It can be observed that the sorption capacities of CRH, NRH, HRH and SRH increased with an increase in the contact time. It can also be observed that acid modification decreased the MB sorption capacities of CRH from 2.43 to 1.65, 1.47 and 1.36 for NRH, HRH and

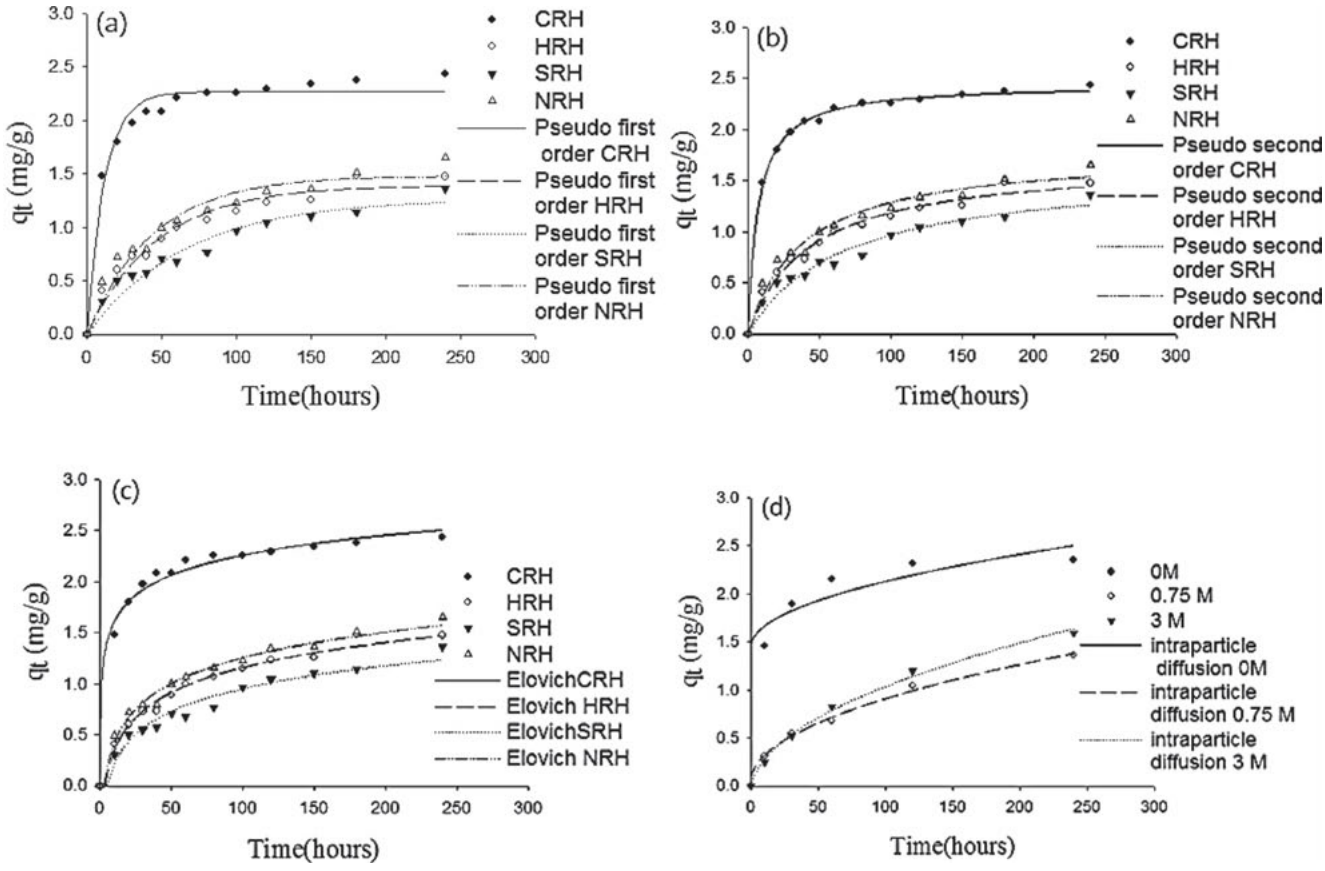

Fig. 4. Comparison between the measured and modeled time profiles and comparison of kinetic models in predicting q_t for the adsorption of MB onto various pretreated rice husks.

SRH, respectively. The results showed that HRH and SRH had the lowest sorption capacity for MB among the modified rice husks. These results indicated that the chemical treatment did not improve the adsorption performance of the rice husks. In fact, modification of CRH could damage the structure of the adsorption surface and affect the mechanisms of adsorption.

In order to design a fast and effective model, further investigations into the adsorption rate were made. A suitable model was sought to understand the mechanisms of adsorption, including the mass transfer chemical reaction [29]. T The experimental data for the uptake of dye versus time, q_t, were fitted to the pseudo-first-order kinetic, pseudo-second-order kinetic, Elovich, and intraparticle diffusion kinetic models using nonlinear regression. The regression results are presented in Fig. 4 and Table 2. Fig. 4a shows a non-linearized plot of the pseudo-first-order model at 50 mg/l initial MB concentration for the first 240 min. It can still be seen from the plots of q_t versus t that the theoretically generated curves do not agree well with the experimental data. This suggests that the sorption of MB onto CRH and acid-modified rice husks does not follow the pseudo-first-order sorption rate expression of Lagergren.

The experimental data and the simulations using the pseudo-second-order equation for adsorption of MB onto different absorbents are shown in Fig. 4b. It shows good agreement with the pseudo-second-order equation, reflected in the extremely high correlation coefficients listed in Table 2, which are greater than 0.96. These findings suggest that the pseudo-second-order kinetic model could be used to predict the amounts of dye taken up at different contact time intervals and at equilibrium.

The simulations using the Elovich equation are plotted in Fig. 4c together with the experimental data points. Table 2 lists the kinetic constants obtained. As can be seen, the constant α was observed to decrease sharply when the CRH was modified by acids, and the constant β also decreased. Therefore, when the CRH is acid-modified within the range studied, the rate of chemisorption and the available adsorption sites on the surface decrease. Although the Elovich equation does not provide any mechanistic evidence, it has proved

Table 2
Kinetic parameters of the removal of MB from aqueous solution by various pretreated rice husks

Adsorbents	Pseudo-first-order			Pseudo-second-order				Elovich equation			Intraparticle diffusion		
	$K1$	q_e	r^2	$K2$	q_e	h	r^2	α	β	r^2	K_{id}	C	r^2
CRH	0.0855	2.2659	0.9730	0.0583	2.4457	0.3490	0.9977	8.6363	3.5569	0.944	0.0653	1.5575	0.8071
HRH	0.0213	1.3907	0.9592	0.0137	1.6983	0.0394	0.9805	0.0946	2.8382	0.9746	0.088	0.2288	0.9609
SRH	0.0152	1.2635	0.9438	0.0094	1.6093	0.0243	0.9642	0.0623	3.1118	0.9408	0.0825	0.0838	0.9815
NRH	0.0227	1.4806	0.9416	0.0144	1.786	0.0453	0.9723	0.1153	2.7588	0.9720	0.091	0.2899	0.9754

suitable for highly heterogeneous systems, of which the adsorption of MB onto CRH, NRH, HRH and SRH is undoubtedly such a case. Moreover, when using the Elovich equation, the correlation coefficients were lower than those of the pseudo-second-order equation, but the Elovich equation might still be used to describe the kinetics of adsorption of MB onto NRH, HRH, and SRH.

The simulations using the intraparticle diffusion equation for the adsorption of MB onto different absorbents are shown in Fig. 4d. As can observed, the intraparticle diffusion model expression does not give a good fit to the experimental data for the adsorption of CRH. This suggests the intraparticle diffusion model cannot be used to predict the amounts of dye taken up at different contact time intervals and at equilibrium for the CRH. However, the intraparticle diffusion equation gives a good fit to the experimental data for the acid-modified rice husks, almost as good as the pseudo-second-order model. Intraparticle diffusion rate constants for CRH, NRH, HRH and SRH were obtained from the plots of the amount of dye adsorbed versus $t^{0.5}$ (Fig. 5). The figure indicates that the adsorption processes for CRH were not linear over the whole time range, and tended to occur in two stages. At a certain time limit for the intraparticle diffusion for the acid-modified absorbents, the curves reveal linear characteristics (as illustrated in Fig. 5). It has been suggested that if the plot of q_t versus $t^{0.5}$ is a straight line, intraparticle diffusion controls the sorption process. If the line does not pass through the origin, the intraparticle diffusion is not the only rate-limiting step, suggesting the process is 'complex', with more than one mechanism limiting the rate of sorption. Though the plots of q_t versus $t^{0.5}$ give straight lines in acid-modified absorbents, they fail to pass through the origin. This might also indicate a combined mass transport triggered by the initial film [39].

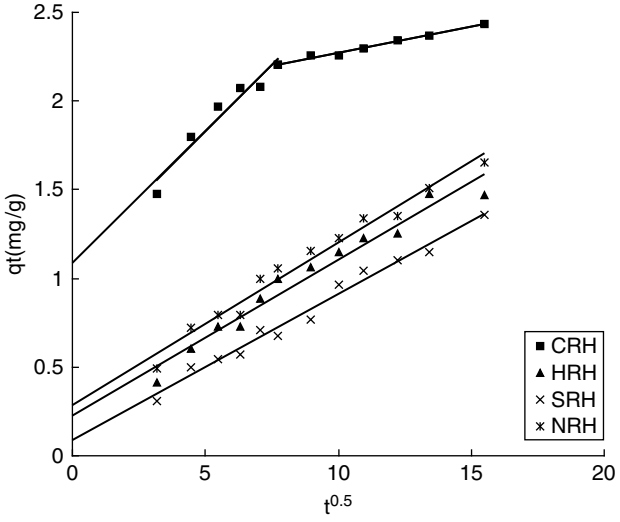

Fig. 5. Intraparticle-diffusion plot for the adsorption of MB onto various pretreated rice husks.

3.4. Effect of MB initial concentration and sorption kinetics

Fig. 6 shows the effect of the initial MB concentration and the contact time on the amount of MB adsorbed onto the CRH. It can be observed that the amount adsorbed increased with contact time, and at a certain point in time reached an almost constant value, with the amount of dye being removed from the aqueous solution onto the CRH in a state of dynamic equilibrium with the amount of dye being desorbed from the CRH into the aqueous solution. As seen in Fig. 6, the initial dye concentrations influenced the contact time necessary to reach the maximum sorption capacities. For the range of contact times under which the experiments were conducted, the adsorption rate for the lower initial MB concentrations was faster than for the higher initial MB concentrations. The adsorption of MB onto CRH was also investigated in terms of the kinetics of the adsorption mechanism by using the pseudo-first-order kinetic, pseudo-second-order kinetic, Elovich, and intraparticle diffusion models.

The fittings of the experimental kinetic results to the pseudo-first-order kinetic models are shown in Fig. 6a, and the values of the estimated parameters are presented in Table 3. It is clear that the theoretically generated curves do not agree well with the experimental data at initial dye concentrations higher than 25 mg/l. This finding suggests that the sorption of MB onto CRH did

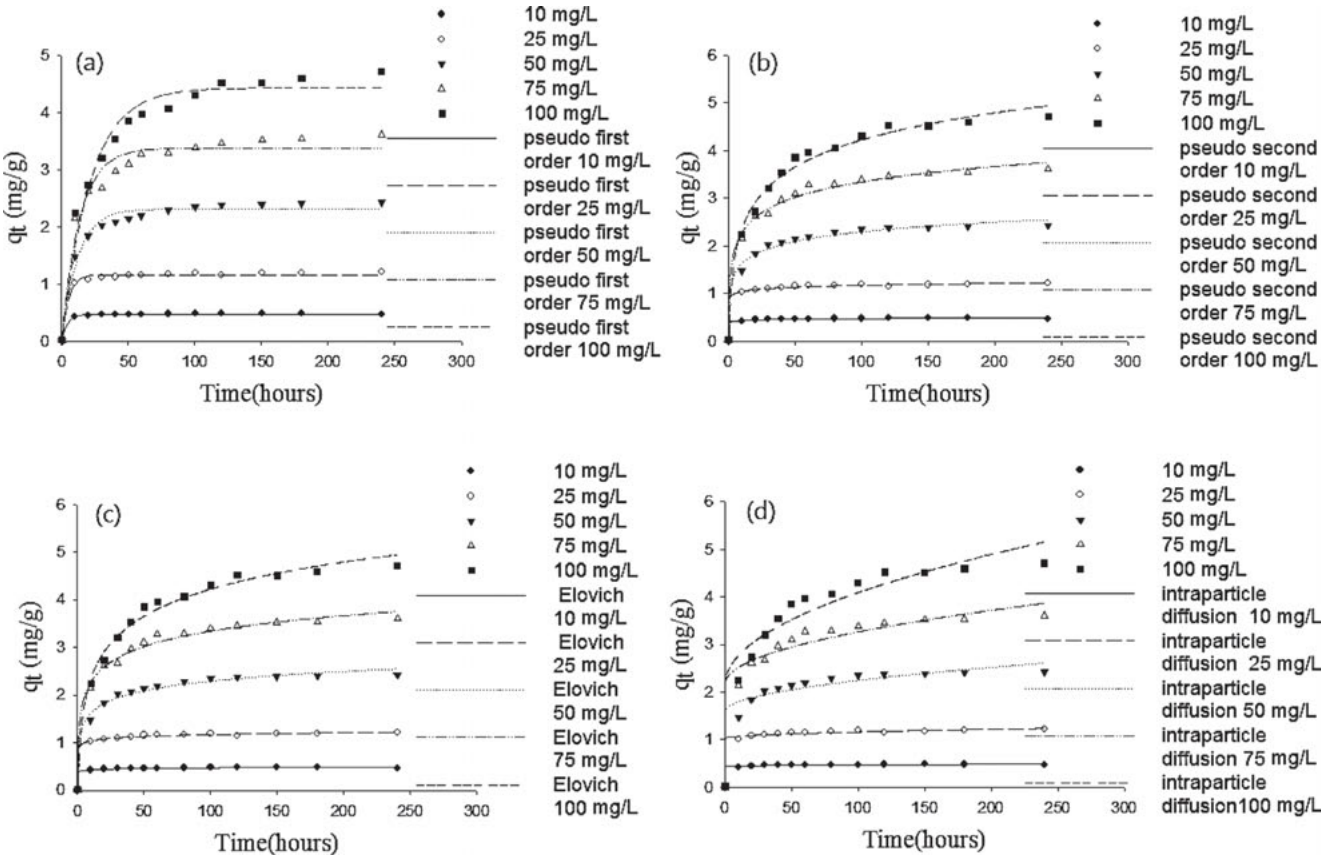

Fig. 6. Comparison between the measured and modeled time profiles and comparison of kinetic models in predicting q_t for the adsorption of MB onto CRH at different initial MB concentrations.

not follow the pseudo-first-order sorption rate expression of Lagergren at high initial MB concentrations.

The pseudo-second-order kinetic constants for adsorption of MB onto CRH are shown in Table 3. The correlation coefficients for the pseudo-second-order kinetic model were close to 1.0 for all cases. In addition, the experimental data and the simulations using the pseudo-second-order kinetic equation for the adsorption of MB onto CRH are shown in Fig. 6b. By comparing Figs. 6a and 6b, it is obvious that for the entire adsorption period the pseudo-second-order model fits the experimental data better than the pseudo-first-order model. This indicates that the sorption mechanism for CRH is chemisorption, involving covalent forces through sharing or exchange of electrons between sorbent and sorbate [64]. Fig. 6b also shows that the calculated q values increased with increasing concentration of MB, presumably due to the enhanced mass transfer of MB molecules to the surface of CRH. This observation suggests that the boundary layer resistance was not the rate limiting step [65].

The experimental data and the simulations using the Elovich equation for the adsorption of MB onto CRH are shown in Fig. 6c. It is clear that the theoretically generated curves agree well with the experimental data at concentrations lower than 25 mg/l, but deviation is observed at later periods of the sorption process at concentration higher than 25 mg/l. Table 3 lists the kinetic constants obtained from the Elovich equation. When using the Elovich equation, the correlation coefficients were lower than those of the pseudo-second-order equation, but it might still be used to describe the kinetics of adsorption of lower initial MB concentrations onto CRH. As can be seen from Table 3, the constants α and β decreased sharply when the initial dye concentrations increased.

The fittings of the experimental kinetic results to the simulations using the intraparticle diffusion kinetic model are shown in Fig. 6d. The intraparticle diffusion model does not fit well to the experimental data for the adsorption of MB. This suggests the intraparticle diffusion model cannot be used to predict the amounts of dye taken up at different contact time intervals and at equilibrium for the CRH.

The intraparticle diffusion plots of the experimental results of q_t versus $t^{0.5}$ for the various absorbents are

Table 3
Kinetic parameters for the effects of initial dye concentrations on sorption of MB onto CRH

MB Concentration	Pseudo-first-order			Pseudo-second-order				Elovich equation			Intraparticle diffusion		
	$K1$	q_e	r^2	$K2$	q_e	h	r^2	α	β	r^2	K_{id}	C	r^2
10 mg/l	0.2302	0.4703	0.9965	1.6354	0.48	0.3768	0.9993	2.07E+08	58.480	0.906	0.002	0.452	0.513
25 mg/l	0.1949	1.1619	0.9885	0.4143	1.1992	0.5959	0.9976	2.71E+05	17.007	0.908	0.011	1.057	0.806
50 mg/l	0.0833	2.3078	0.9764	0.0555	2.4949	0.3453	0.9989	5.2531	3.202	0.947	0.040	1.871	0.854
75 mg/l	0.0739	3.3767	0.9586	0.0326	3.6728	0.4400	0.9930	4.62877	2.032	0.964	0.091	2.380	0.851

shown in Fig. 7. Within these, the first, sharper region is the instantaneous adsorption or external surface adsorption. The second region is the gradual adsorption stage where intraparticle diffusion is rate limiting. In some cases, a third region exists, the final equilibrium stage where intraparticle diffusion starts to slow down due to the extremely low adsorbate concentrations left in the solutions [66]. The plots in Fig. 7 are not linear over the whole time range, implying that more than one process affected the adsorption. This indicates that the rate of adsorption for the initial MB concentrations of 10, 25, 50, 75, and 100 mg/l was initially controlled by film diffusion, then changed to intraparticle-diffusion control after 50–60 min. The intercepts (C) and the intraparticle rate constant (K_{id}) values calculated from the slopes of the linear portions of the plots of Fig. 7 are presented in Table 3. The intercept C provides information about the thickness of the boundary layer; the resistance to the external mass transfer increases as the intercept increases. The constant C was found to increase from 0.4393 to 2.171 with an increase in the dye concentration from 10 to 75 mg/l, indicating an increase in the thickness of the boundary layer and a decrease in the chance of external mass transfer, and hence an increase in the chance of internal mass transfer [67]. However, beyond 75 mg/l, the intercept decreased, suggesting that at higher concentrations, the sorption process is controlled by intraparticle diffusion, with only a minor effect from the external film. Ponnusami et al. reported a similar observation for the adsorption of MB onto guava (*Psidium guajava*) leaf powder [68]. The value of K_{id} was found to increase with an increasing initial concentration of dye solution. Another similar observation was reported by Mane et al. for the adsorption of brilliant green onto bagasse fly ash [69].

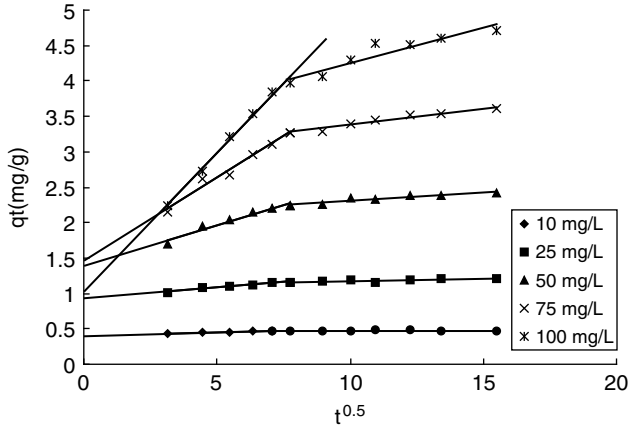

Fig. 7. Intraparticle diffusion plot for the adsorption of MB onto CRH at different initial MB concentrations.

3.5. Adsorption isotherms

The capacity of CRH for adsorption of MB can be determined by measuring equilibrium isotherms, which describe how adsorbates interact with adsorbents. The correlation of equilibrium data to either theoretical or empirical equations is essential for the subsequent practical application of the isotherms [50]. Several mathematical models can be used to describe experimental data for adsorption isotherms. The experimental data were analyzed according to the nonlinear forms of the Langmuir, Freundlich, Temkin, Redlich–Peterson, and Langmuir–Freundlich empirical models. Table 4 gives the calculated isotherm constants for the different initial MB concentrations. In order to assess the different isotherms and their ability to correlate the experimental results, the theoretical plots for each isotherm have been shown along with the experimental data for the adsorption of MB onto CRH (Fig. 8). The isotherm curves show the superposition of the experimental results (points) and the theoretical calculated results (lines).

The Langmuir sorption model serves to estimate the maximum uptake or the total capacity of the adsorbent for the dye (q_{max}) where it could not be reached in the experiments. K_L is the adsorption equilibrium constant representing the affinity between the sorbent and sorbate. The values of q_{max} and K_L calculated from the Langmuir model are tabulated in Table 4. The calculated R_L values versus the initial MB concentrations are shown in Fig. 9, in which it can be observed that sorption was more favorable at higher concentrations.

Table 4
Isotherm parameters for MB adsorption onto CRH

Langmuir	q_{max}(mg/g)	8.07
	K_L (l/mg)	0.1414
	r^2	0.9986
Freundlich	K_F (mg$^{1-(1/n)}$ $L^{1/n}$g^{-1})	1.1211
	n	1.5588
	r^2	0.9822
Temkin	A_T(l/g)	2.6083
	B_T	1946.309
	r^2	0.9608
Redlich–Peterson	K_R (l/g)	1.141
	A ((l/mg)^b)	0.1414
	B	0.9999
	r^2	0.9986
Langmuir–Freundlich	K_{LF}((l/mg)$^{1/n}$)	0.1598
	q_{LF}(mg/g)	6.7459
	$1/n$	1.151
	r^2	0.9999

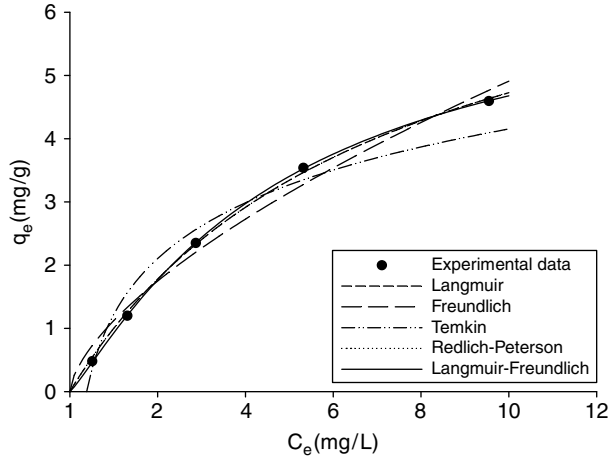

Fig. 8. Experimental points and comparison of the fitted curves from various adsorption isotherms for the adsorption of MB onto CRH.

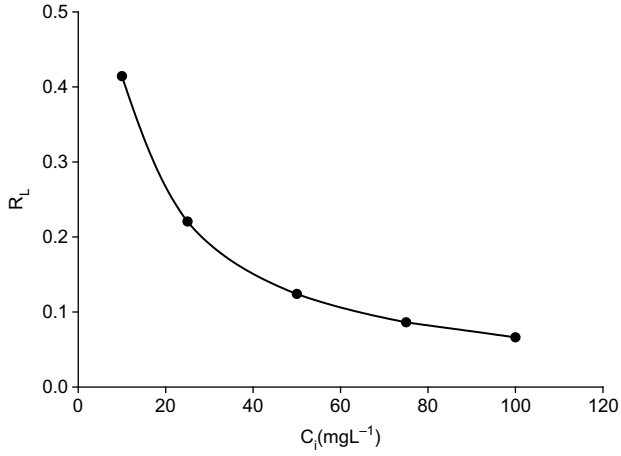

Fig. 9. Plot of the separation factor for MB onto CRH versus the initial dye concentration.

Table 5
Comparison of adsorption capacities of various adsorbents for methylene blue

Adsorbent	q_m (mg/g)	References
Glass wool	0.0243–2.2436	72
Guava seeds activated carbon	0.667–0.625	71
Activated carbon from Almond shell	1.33	73
Caulerpa racemosa var. *cylindracea*	2.471–5.233	13
Fly ash	2.755–3.074	74
Activated carbon from Walnut shell	3.53	73
Neem leaf powder	3.67–19.61	75
Activated carbon from Apricot stones	4.11	73
Clay	4.4–6.3	76
Raw *P. oceanica* fibres	5.56	37
Coir pith activated carbon	5.87	77
Rice Husk	8.07	This study
Activated carbon from Hazelnut shell	8.82	73

The fact that R_L is in the range of 0–1 at all initial dye concentrations confirms the favorable uptake of the malachite green process [70]. Table 5 presents a comparison of the adsorption capacity of the CRH obtained in this study with those obtained in the literature for the adsorption of MB. It shows that CRH can be considered as a promising material for removing basic dyes, even compared to some other low cost adsorbents and activated carbons previously suggested for the uptake of MB from aqueous solutions [13, 37, 71–77].

The Freundlich isotherm was originally empirical in nature but was later interpreted for sorption to heterogeneous surfaces or surfaces supporting sites of varied affinities and has been used widely to fit experimental data [78]. The value of n, the Freundlich constant, is an empirical parameter that varies with the degree of heterogeneity and indicates the degree of non-linearity between dye uptake capacity and unadsorbed dye in the solution, and is related to the distribution of bonded ions on the sorbent surface [79]. In general, an $n > 1$ suggests that the adsorbate is favorably adsorbed onto an adsorbent. The results in Table 4 indicate that MB was favorably adsorbed by CRH, as the n value was greater than one. Compared to the Langmuir isotherm, the Freundlich isotherm had a poorer fit to the present data.

The Temkin constants A_T and B_T are listed in Table 4 and the theoretical plot of this isotherm is shown in

Fig. 8. The correlation coefficient is also given in Table 4 and is lower than the Langmuir and Freundlich values. Therefore, the Langmuir and Freundlich isotherms fit better to the experimental data than the Temkin isotherm. Fig. 8 shows the same.

The experimental data were further fitted to the three-parameter Redlich-Peterson isotherm and Langmuir–Freundlich isotherm models. The three-parameter empirical Redlich-Peterson isotherm equation combines elements from both the Langmuir and Freundlich equations, modeling a hybrid mechanism of adsorption is a hybrid, not following ideal monolayer adsorption. Therefore, the Redlich–Peterson isotherm equation is widely used as a compromise between the Langmuir and Freundlich systems. The adsorption parameters calculated according to the Redlich–Peterson isotherm model are listed in Table 4. The r^2 was higher than 0.998, while b was smaller than one, obeying the theory behind the Redlich-Peterson isotherm. In fact, any value of b out of the range 0–1 fails to agree with the theory behind the Redliche-Peterson isotherm. Fig. 8 illustrates that the Redlich–Peterson isotherm model is a better fit to the experimental data than the Freundlich and Temkin isotherms.

The Langmuir–Freundlich model is another three-parameter empirical model for representing equilibrium biosorption data. It is also a combination of the Langmuir and Freundlich isotherm type models. The corresponding Langmuir–Freundlich parameters of A, B and m are given in Table 4 and the theoretical plot is shown in Fig. 8. As seen from Table 4 and Fig. 8, the Langmuir–Freundlich isotherm provides the best correlation to the experimental data, whereas Langmuir and Redlich–Peterson isotherms also fitted the experimental data.

4. Conclusions

1. The experimental results indicated that both untreated and acid-modified rice husks show promise as adsorbents for the removal of MB from aqueous solutions.
2. The chemical modification of rice husks to produce NRH, HRH and SRH reduced the sorption efficiency of CRH for MB from 98% to 67%, 59% and 55%, respectively.
3. The sorption capacity increased with higher initial dye concentrations. It is speculated that the initial concentration of dye provides the driving force to overcome the resistances to the mass transfer of MB between the aqueous and the solid phases. In addition, an increase in the initial dye concentration enhances the interactions between MB and the CRH. An increase in the initial MB dye concentration enhances the adsorption of MB.
4. The sorption data were found to follow the pseudo-second-order kinetic model.
5. The q_t versus $t^{1/2}$ plots NRH, HRH and SRH give a straight line, but do not pass through the origins. This indicates a combined mass transport triggered by initial film mass transfer followed by intraparticle diffusion. The results also indicate that the acid modification of CRH can destroy the structure of the adsorption surface, affecting the adsorption boundary layer and decreasing the contribution of the surface sorption in the rate-controlling step.
6. The analysis indicates that the adsorption of CRH does not occur on a heterogeneous surface with sites of equivalent energy of adsorption that are always available, since the Freundlich isotherm had a poor fit to the experimental data.
7. The experimental adsorption data fitted better to the Langmuir–Freundlich model than the other models.

References

[1] C. Namasivayam and D. Kavitha, Removal of Congo Red from water by adsorption onto activated carbon prepared from coir pith, an agricultural solid waste, Dyes Pigm., 54 (2002) 47–58.
[2] I.D. Mall, V.C. Srivastava, N.K. Agarwal and I.M. Mishra, Removal of congo red from aqueous solution by bagasse fly ash and activated carbon: Kinetic study and equilibrium isotherm analyses, Chemosphere, 61 (2005) 492–501.
[3] Z. Aksu, S. Tezer, Equilibrium and kinetic modelling of biosorption of Remazol Black B by Rhizopus arrhizus in a batch system: effect of temperature, Process Biochem., 36 (2000) 431–439.
[4] A. Ozer, G. Akkaya and M. Turabik, Biosorption of Acid Blue 290 (AB 290) and Acid Blue 324 (AB 324) dyes on Spirogyra rhizopus, J. Hazard. Mater., 135 (2006) 355–364.
[5] G. Aggelis, C. Ehaliotis, F. Nerud, I. Stoychev, G. Lyberatos and G.I. Zervakis, Evaluation of white-rot fungi for detoxification and decolorization of effluents from the green olive debittering process, Appl. Microbiol. Biotechnol., 59 (2002) 353–360.
[6] T. Robinson, B. Chandran and P. Nigam, Studies on desorption of individual textile dyes and a synthetic dye effluent from dye-adsorbed agricultural residues using solvents, Bioresour. Technol., 84 (2002) 299–301.
[7] T. Robinson, G. McMullan, R. Marchant and P. Nigam, Remediation of dyes in textile effluent: a critical review on current treatment technologies with a proposed alternative, Bioresour. Technol., 77 (2001) 247–255.
[8] C.I. Pearce, J.R. Lloyd and J.T. Guthrie, The removal of colour from textile wastewater using whole bacterial cells: a review, Dyes Pigm., 58 (2003) 179–196.
[9] K.C. Chen, J.Y. Wu, D.J. Liou and S.C.J. Hwang, Decolorization of the textile dyes by newly isolated bacterial strains, J. Biotechnol., 101 (2003) 57–68.
[10] S. Wang and Z.H. Zhu, Characterisation and environmental application of an Australian natural zeolite for basic dye removal from aqueous solution, J. Hazard. Mater., 136 (2006) 946–952.
[11] M. Otero, F. Rozada, L.F. Calvo and A.I. Garcia, A. Moran, Kinetic and equilibrium modelling of the methylene blue removal from solution by adsorbent materials produced from sewage sludges, Biochem. Eng. J., 15 (2003) 59–68.
[12] Y. Fu and T. Viraraghavan, Column studies for biosorption of dyes from aqueous solutions on immobilised Aspergillus niger fungal biomass, Water S. A., 29 (2003) 465–472.
[13] S. Cengiz and L. Cavas, Removal of methylene blue by invasive marine seaweed: Caulerpa racemosa var. cylindracea, Bioresour. Technol., 99 (2008) 2357–2363.

[14] G. McKay, J.F. Porter and G.R. Prasad, The Removal of Dye Colours from Aqueous Solutions by Adsorption on Low-cost Materials, Water Air Soil Pollut., 114 (1999) 423–438.
[15] Y. Bulut and H. Ayd?n, A kinetics and thermodynamics study of methylene blue adsorption on wheat shells, Desalination, 194 (2006) 259–267.
[16] R. Gong, S. Zhu, D. Zhang, J. Chen, S. Ni and R. Guan, Adsorption behavior of cationic dyes on citric acid esterifying wheat straw: kinetic and thermodynamic profile, Desalination, 230 (2008) 220–228.
[17] A. Ozer and G. Dursun, Removal of methylene blue from aqueous solution by dehydrated wheat bran carbon, J. Hazard. Mater., 146 (2007) 262–269.
[18] K.V. Kumar, Adsorption isotherms for basic dyes onto low cot adsorbents, Res. J. Chem. Environ., 6 (2002) 61–65.
[19] Y.S. Ho, T.H. Chiang and Y.M. Hsueh, Removal of basic dye from aqueous solution using tree fern as a biosorbent, Process Biochem., 40 (2005) 119–124.
[20] T. Robinson, B. Chandran and P. Nigam, Removal of dyes from a synthetic textile dye effluent by biosorption on apple pomace and wheat straw, Water Res., 36 (2002) 2824–2830.
[21] I. Bouzaida and M.B. Rammah, Adsorption of acid dyes on treated cotton in a continuous system, Mater. Sci. Eng. C, 21 (2002) 151–155.
[22] K.V. Kumar and A. Kumaran, Removal of methylene blue by mango seed kernel powder, Biochem. Eng. J., 27 (2005) 83–93.
[23] H. Aydin and G. Baysal, Adsorption of acid dyes in aqueous solutions by shells of bittim (Pistacia khinjuk Stocks), Desalination, 196 (2006) 248–259.
[24] B.H. Hameed, D.K. Mahmoud and A.L. Ahmad, Sorption equilibrium and kinetics of basic dye from aqueous solution using banana stalk waste, J. Hazard. Mater., (2008).
[25] G.M. Walker, L. Hansen, J.A. Hanna and S.J. Allen, Kinetics of a reactive dye adsorption onto dolomitic sorbents, Water Res., 37 (2003) 2081–2089.
[26] Y.C. Wong, Y.S. Szeto, W.H. Cheung and G. McKay, Adsorption of acid dyes on chitosan—equilibrium isotherm analyses, Process Biochem., 39 (2004) 695–704.
[27] A.E. Ofomaja, Kinetic study and sorption mechanism of methylene blue and methyl violet onto mansonia (Mansonia altissima) wood sawdust, Chem. Eng. J., (2008) 85–95.
[28] A.E. Ofomaja, Sorptive removal of Methylene blue from aqueous solution using palm kernel fibre: Effect of fibre dose, Biochem. Eng. J., (2008) 8–18.
[29] S. Senthilkumaar, P.R. Varadarajan, K. Porkodi and C.V. Subbhuraam, Adsorption of methylene blue onto jute fiber carbon: kinetics and equilibrium studies, J. Colloid Interface Sci., 284 (2005) 78–82.
[30] B. Acemioglu, Batch kinetic study of sorption of methylene blue by perlite, Chem. Eng. J., 106 (2005) 73–81.
[31] D. Ghosh and K.G. Bhattacharyya, Adsorption of methylene blue on kaolinite, Appl. Clay Sci., 20 (2002) 295–300.
[32] A. Al-Futaisi, A. Jamrah and R. Al-Hanai, Aspects of cationic dye molecule adsorption to palygorskite, Desalination, 214 (2007) 327–342.
[33] B. Armağan, M. Turan and M.S. lik, Equilibrium studies on the adsorption of reactive azo dyes into zeolite, Desalination, 170 (2004) 33–39.
[34] H.D. Choi, M.C. Shin, D.H. Kim, C.S. Jeon and K. Baek, Removal characteristics of reactive black 5 using surfactant-modified activated carbon, Desalination, 223 (2008) 290–298.
[35] A.A.M. Daifullah, B.S. Girgis and H.M.H. Gad, Utilization of agro-residues (rice husk) in small waste water treatment plans, Mater. Lett., 57 (2003) 1723–1731.
[36] R. Djeribi and O. Hamdaoui, Sorption of copper (II) from aqueous solutions by cedar sawdust and crushed brick, Desalination, 225 (2008) 95–112.
[37] M.C. Ncibi, B. Mahjoub and M. Seffen, Kinetic and equilibrium studies of methylene blue biosorption by Posidonia oceanica (L.) fibres, J. Hazard. Mater., 139 (2007) 280–285.
[38] A. Gunay, E. Arslankaya and I. Tosun, Lead removal from aqueous solution by natural and pretreated clinoptilolite: Adsorption equilibrium and kinetics, J. Hazard. Mater., 146 (2007) 362–371.
[39] S. Ayoob, A.K. Gupta, P.B. Bhakat and V.T. Bhat, Investigations on the kinetics and mechanisms of sorptive removal of fluoride from water using alumina cement granules, Chem. Eng. J., 140 (2008) 6–14.
[40] Y. Ho and G. McKay, A comparison of chemisorption kinetic models applied to pollutant removal on various sorbents, Process safety and environmental protection: transactions of the Institution of Chemical Engineers, Part B, 76 (1998) 332–340.
[41] E. Demirbas, M. Kobya, E. Senturk and T. Ozkan, Adsorption kinetics for the removal of chromium(VI) from aqueous solutions on the activated carbons prepared from agricultural wastes, Water S. A., 30 (2004) 533–540.
[42] O. Neşe and K.T. Ennil, A kinetic study of nitrite adsorption onto sepiolite and powdered activated carbon, Desalination, 223 (2008) 174–179.
[43] N. Yeddou and A. Bensmaili, Equilibrium and kinetic modelling of iron adsorption by eggshells in a batch system: effect of temperature, Desalination, 206 (2007) 127–134.
[44] A.A. Augustine, B.D. Orike and A.D. Edidiong, Adsorption kinetics and modeling of cu(II) ion sorption from aqueous solution by mercaptoacetic acid modified cassava (manihot sculenta cranz) wastes, EJEAFChe, 6 (2007) 2221–2234.
[45] S.H. Chien and W.R. Clayton, Application of Elovich Equation to the Kinetics of Phosphate Release and Sorption in Soils, Soil Sci. Soc. Am. J., 44 (1980) 265–268.
[46] B.H. Hameed and M.I. El-Khaiary, Sorption kinetics and isotherm studies of a cationic dye using agricultural waste: Broad bean peels, J. Hazard. Mater., (2008) 639–648.
[47] M. Alkan, M. Doğan, Y. Turhan, O. Demirba and P. Turan, Adsorption kinetics and mechanism of maxilon blue 5G dye on sepiolite from aqueous solutions, Chem. Eng. J., 139 (2008) 213–223.
[48] Y. Onal, Kinetics of adsorption of dyes from aqueous solution using activated carbon prepared from waste apricot, J. Hazard. Mater., 137 (2006) 1719–1728.
[49] W.J. Weber and J.C. Morris, Kinetics of adsorption on carbon from solution, J. Sanit. Eng. Div. Am. Soc. Civ. Eng., 89 (1963) 31–60.
[50] E.N. El Qada, S.J. Allen and G.M. Walker, Adsorption of Methylene Blue onto activated carbon produced from steam activated bituminous coal: A study of equilibrium adsorption isotherm, Chem. Eng. J., 124 (2006) 103–110.
[51] R. Han, Y. Wang, P. Han, J. Shi, J. Yang and Y. Lu, Removal of methylene blue from aqueous solution by chaff in batch mode, J. Hazard. Mater., 137 (2006) 550–557.
[52] A. Sari, M. Tuzen, D. Citak and M. Soylak, Equilibrium, kinetic and thermodynamic studies of adsorption of Pb (II) from aqueous solution onto Turkish kaolinite clay, J. Hazard. Mater., 149 (2007) 283–291.
[53] M. Imamoglu and O. Tekir, Removal of copper (II) and lead (II) ions from aqueous solutions by adsorption on activated carbon from a new precursor hazelnut husks, Desalination, 228 (2008) 108–113.
[54] M. Dogan, M. Alkan, A. Turkyilmaz and Y. Ozdemir, Kinetics and mechanism of removal of methylene blue by adsorption onto perlite, J. Hazard. Mater., 109 (2004) 141–148.
[55] E. Oguz, Equilibrium isotherms and kinetics studies for the sorption of fluoride on light weight concrete materials, Colloids Surf., A, 295 (2007) 258–263.
[56] Z. Al-Qodah, A.T. Shawaqfeh and W.K. Lafi, Adsorption of pesticides from aqueous solutions using oil shale ash, Desalination, 208 (2007) 294–305.
[57] O. Hamdaoui and E. Naffrechoux, Modeling of adsorption isotherms of phenol and chlorophenols onto granular activated carbon Part II. Models with more than two parameters, J. Hazard. Mater., 147 (2007) 401–411.

[58] M. Sathishkumar, A.R. Binupriya, K. Vijayaraghavan and S.I. Yun, Two and three-parameter isothermal modeling for liquid-phase sorption of Procion Blue HB by inactive mycelial biomass of Panus fulvus, J. Chem. Technol. Biotechnol., 82 (2007) 389–398.
[59] V.J.P. Vilar, C.M.S. Botelho and R.A.R. Boaventura, Copper removal by algae Gelidium, agar extraction algal waste and granulated algal waste: Kinetics and equilibrium, Bioresour. Technol., 99 (2008) 750–762.
[60] C. Teixeira Tarley, S. Costa Ferreira and M. Zezzi Arruda, Use of modified rice husks as a natural solid adsorbent of trace metals: characterisation and development of an on-line preconcentration system for cadmium and lead determination by FAAS, Microchem. J., 77 (2004) 163–175.
[61] E. Chockalingam, K. Sivapriya, S. Subramanian and S. Chandrasekaran, Rice husk filtrate as a nutrient medium for the growth of Desulfotomaculum nigrificans: characterisation and sulfate reduction studies, Bioresour. Technol., 96 (2005) 1880–1888.
[62] S. Javed, S. Naveed, N. Feroze, M. Zafar and M. Deary, Quality Improvement of Amorphous Silica by Using $KMnO_4$, J. Qual. Technol. Manage., 4 (2008).
[63] A.B. Perez-Marin, V.M. Zapata, J.F. Ortuno, M. Aguilar, J. Saez and M. Llorens, Removal of cadmium from aqueous solutions by adsorption onto orange waste, J. Hazard. Mater., 139 (2007) 122–131.
[64] Y.S. Ho and G. McKay, Pseudo-second order model for sorption processes, Process Biochem., 34 (1999) 451–465.
[65] R. Patel and S. Suresh, Kinetic and equilibrium studies on the biosorption of reactive black 5 dye by Aspergillus foetidus, Bioresour. Technol., 99 (2008) 51–58.
[66] B.H. Hameed, R.R. Krishni and S.A. Sata, A novel agricultural waste adsorbent for the removal of cationic dye from aqueous solutions, J. Hazard Mater., 2008.
[67] A.E. Nemr, O. Abdelwahab, A. El-Sikaily and A. Khaled, Removal of direct blue–86 from aqueous solution by new activated carbon developed from orange peel, J. Hazard. Mater., (2008).
[68] V. Ponnusami, S. Vikram and S.N. Srivastava, Guava (Psidium guajava) leaf powder: Novel adsorbent for removal of methylene blue from aqueous solutions, J. Hazard. Mater., 152 (2008) 276–286.
[69] V.S. Mane, I.D. Mall and V.C. Srivastava, Use of bagasse fly ash as an adsorbent for the removal of brilliant green dye from aqueous solution, Dyes Pigm., 73 (2007) 269–278.
[70] O. Hamdaoui, F. Saoudi, M. Chiha and E. Naffrechoux, Sorption of malachite green by a novel sorbent, dead leaves of plane tree: Equilibrium and kinetic modeling, Chem. Eng. J., 143 (2008) 73–84.
[71] I.A. Rahman and B. Saad, Utilization of Guava Seeds as a Source of Activated Carbon for Removal of Methylene Blue from Aqueous Solution, Malays. J. Chem., 5 (2003) 8–14.
[72] S. Chakrabarti and B.K. Dutta, On the adsorption and diffusion of Methylene Blue in glass fibers, J. Colloid Interface Sci., 286 (2005) 807–811.
[73] A. Aygun, S. Yenisoy-Karaka and I. Duman, Production of granular activated carbon from fruit stones and nutshells and evaluation of their physical, chemical and adsorption properties, Microporous Mesoporous Mater., 66 (2003) 189–195.
[74] V.V. Basava Rao and S. Ram Mohan Rao, Adsorption studies on treatment of textile dyeing industrial effluent by flyash, Chem. Eng. J., 116 (2006) 77–84.
[75] K.G. Bhattacharyya and A. Sharma, Kinetics and thermodynamics of methylene blue adsorption on Neem (Azadirachta indica) leaf powder, Dyes Pigm., 65 (2005) 51–59.
[76] A. Gürses, S. Karaca, C. Doğar, R. Bayrak, M. Açıkyıldız and M. Yalcin, Determination of adsorptive properties of clay/water system: methylene blue sorption, J. Colloid Interface Sci., 269 (2004) 310–314.
[77] D. Kavitha and C. Namasivayam, Experimental and kinetic studies on methylene blue adsorption by coir pith carbon, Bioresour. Technol., 98 (2007) 14–21.
[78] S. Basha, Z.V.P. Murthy and B. Jha, Sorption of Hg (II) from Aqueous Solutions onto Carica papaya: Application of Isotherms, Ind. Eng. Chem. Res., 47 (2008) 980–986.
[79] Z. Aksu, A. Tatl and O. Tunc, A comparative adsorption/biosorption study of Acid Blue 161: Effect of temperature on equilibrium and kinetic parameters, Chem. Eng. J., 2007.